First-principles simulation of Se and Te adsorbed on GaAs(001)

S. Gundel* and W. Faschinger

Physikalisches Institut der Universität Würzburg, EP III, Am Hubland, D-97074 Würzburg, Germany

(Received 13 May 1998; revised manuscript received 9 September 1998)

We have studied the adsorption of Se and Te on GaAs(001) using first-principles simulations. For each chalcogen species, 11 structures exhibiting 2×1 reconstruction with varying surface stoichiometry were simulated using a density functional formalism and pseudopotentials, thus yielding absolute surface energies and detailed information about the atomic positions. Our results are discussed in terms of a simple model for heteropolar surfaces and compared to experimental results for these surfaces available from the literature. [S0163-1829(99)07503-7]

I. INTRODUCTION

Experimental results concerning the GaAs(001) surface modified by adsorption of group VI atoms have been used extensively in recent years to establish a microscopic picture of this surface. Structural models proposed to date have been based mainly on scanning tunneling microscopy and photoemission spectroscopy data. The available experimental data concerning the most extensively investigated 2×1 reconstruction formed by chalcogen adsorption on the GaAs(001) surface are used as a starting point for calculations based upon density functional theory which were carried out to determine the energetically favorable structures.

It is evident that the microscopic structure of the adsorbate-covered surface depends strongly upon the sample preparation. The experimental investigations to be reviewed in further detail below agree upon the observation of two distinct bonding sites for both Se and Te on the GaAs(001) surface, as well as the temperature ranges within which the 2×1 reconstruction is formed with each chalcogen species. However, there is disagreement concerning the amount of chalcogen atoms adsorbed on the respective surfaces and also on the microscopic structure of the surface, one of the main issues being whether or not chalcogen dimers are formed in the top atomic layers.

A diagram of surface reconstructions for the case of Se/GaAs prepared by molecular beam epitaxy has been provided by Takatani, Kikawa, and Nakazawa.[1] It shows that within a moderate temperature range, a 2×1 reconstruction will form on a previously As-rich GaAs surface. At temperatures above 550 °C first a 2×3 reconstruction and later a 4×3 reconstruction are seen. From these the 2×1 reconstruction can be obtained by lowering the temperature under Se flux. This diagram has been subsequently confirmed in various investigations. Scimeca et al.[2] state that after depositing Se on a previously 2×4 reconstructed GaAs(001) surface at room temperature and subsequent annealing at 250 °C, the Se atoms are primarily bound to surface As atoms while Se deposition at 580 °C leads to the formation of Se—Ga bonds. Li and Pashley[3] found that a deposition of less than 0.25 monoatomic layers of Se causes the creation of holes in the GaAs surface while further Se deposition leads to the formation of 2×1 reconstructed islands and finally to a smooth and well ordered surface. Chambers and Sundaram[4] report results from sample preparation by metalorganic chemical

vapor deposition and state that depositing H_2Se at 425 °C and annealing at 550 °C yields a sharp 2×1 electron diffraction [low energy electron diffraction (LEED)] pattern for the surface.

In the case of Te adsorption on GaAs, a diagram similar to that in Ref. 1 has been provided by Gobil et al.[5] The 2×1 reconstruction is formed either from the 2×4 reconstructed GaAs surface or via an intermediate 6×1 reconstruction from the $c(4\times4)$ reconstruction of GaAs. At temperatures above 540 °C another 6×1 reconstruction and a $\sqrt{3}\times3$ reconstruction are observed. These findings were confirmed afterwards by Etgens et al.[6] Sugiyama and Maeyama[7] obtained a 2×1 reconstruction by evaporating Te onto GaAs at 450 °C.

Quantitative information about the amount of Se or Te being adsorbed on the 2×1 reconstructed GaAs surface has been derived mainly from photoemission spectroscopy. Biegelsen et al.[8] state that after the formation of the 2×1 reconstruction, one atomic layer of Se has replaced a similar amount of As while the Ga signal remains nearly constant. In the case of Te about half an atomic layer is adsorbed, accompanied by a similar loss of As. In addition Spahn et al.[9] have found that about half of the initially adsorbed atomic layer of Se is replaced by Te during subsequent exposure of the Se/GaAs sample to a Te molecular beam, and have concluded that Se atoms are adsorbed at two nonequivalent bonding sites. A different coverage was found by Scimeca et al.[2] who suggest that about two atomic layers are adsorbed in the vicinity of the GaAs surface, but agree about different bonding sites of Se atoms at and beneath the surface. The investigation by Takatani, Kikawa, and Nakazawa[1] confirms these results. A similar splitting of the Te $3d_{5/2}$ peak is reported by Gobil et al.[5] for the case of Te adsorbed on GaAs. From the peak shifts they conclude that Te atoms are bound to As as well as to other Te atoms. Further quantitative measurements were made by Chambers and Sundaram,[4] who fitted data from x-ray photoelectron diffraction to scattering theory calculations and derived fractional occupation values of the first atomic layers with Se and Te. They state that the occupation values for Se on GaAs are about 0.75, 0.5, and 0.25 for the first, third, and fifth layer, respectively. For Te on GaAs they report occupation values of 1.0, 0.1, and 0 for the same layers.

From scanning tunneling microscopy data, Pashley and

Li[10] have concluded that Se dimers are formed on top of a 2×1 reconstructed Se-adsorbed GaAs surface. They based their conclusion on the height modulation of the tip along the $[1\bar{1}0]$ direction. Starting from this observation and assuming Pashley's electron counting rule[11] to be valid for the Se-adsorbed surface they proposed a structural model which assumes two atomic layers of Se to be adsorbed at As sites in the first and third atomic layers while the additional electrons introduced by the Se atoms require a Ga vacancy at every second site in the fourth layer in order for the electron counting rule to remain valid. Biegelsen *et al.*[8] report rows of dimer-like features along the [011] direction. A recent investigation of Te on GaAs employing x-ray standing wave analysis[7] states that Te atoms also occupy two nonequivalent bonding sites at the GaAs surface while they are situated close to As positions. The authors give detailed information about the locations of these Te atoms and propose a structural model in which the Te atoms in the top layers remain in ideal bridge positions between two Ga atoms and do not form dimers.

At this point *ab initio* calculations can be employed to investigate in detail the stability of the proposed structures. An early first-principles study of group VI atoms on GaAs was done by Ohno.[12] He studied the behavior of one single atom of S, Se, or Te on a 1×1 GaAs surface cell, thus assuming coverage of one atomic layer and neglecting electron counting considerations and possible reconstructions. From his simulations he concluded that chalcogen atoms adsorb preferentially at the bridge site between either two Ga or two As atoms, while the chalcogen—Ga bond appears to be stronger than the chalcogen—As bond. The adsorption energy decreases with increasing mass number of the adsorbed chalcogen atom as expected, but while the adsorption energy for Se in the bridge site is only about 0.4 eV lower than for S, the energies for Se and Te at the same site differ by about 1.2 eV. Ohno suggested further that the nearly filled chalcogen dangling bonds would render the surface resistant to additional adsorption.

The intention of the present work is to report on first-principles pseudopotential calculations which are similar to those of Ohno[12] but take into account the experimentally observed 2×1 reconstruction and strictly adhere to Pashley's electron counting rule for the structures considered in this work. The validity of this latter restriction in the present work is demonstrated by Fig. 1 which depicts on the right-hand side the atomic s and p levels of Ga and As as well as the levels formed by sp^3 hybridization and the valence and conduction band edges of GaAs. On the left-hand side the respective levels for Se and Te are depicted, the data being taken from Harrison.[13] Since the sp^3 hybrid energy levels for both Se and Te are clearly beneath the valence band edge of GaAs, the enforcement of the electron counting rule appears to be justified from the argument presented by Pashley.[11]

Following this line of reasoning, the structure models presented in Refs. 8 and 10 along with the experimental results presented earlier in this Introduction have been used as a guideline in a proposal of 11 structural models of Se and Te adsorbed on the GaAs(001) surface which were subsequently studied by *ab initio* simulations. From the resulting total energies of the supercells, absolute surface energies have been calculated. These surface energies are shown in diagrams as
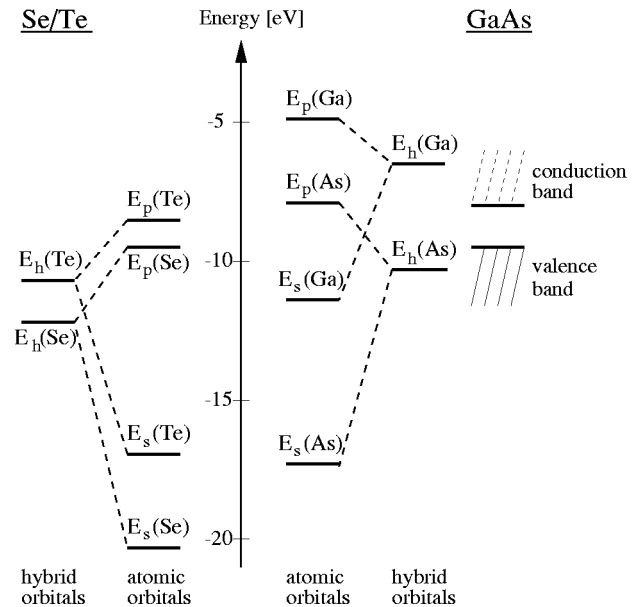

FIG. 1. Atomic and hybrid energy levels of Ga, As, Se, and Te. The data are taken from Harrison.

functions of the chemical potentials of As and the adsorbed chalcogen species, which is either Se or Te.

The paper is organized as follows. In Sec. II the self-consistent calculations that were employed to obtain the total energies of the structures considered are briefly outlined. The equations that allow us to calculate surface energies as a function of two chemical potentials are also presented. In Sec. III the results of our simulations are presented and discussed with an emphasis on their relation to the experimental results summarized in the Introduction. The paper is concluded by a brief summary in Sec. IV.

II. METHOD OF THE CALCULATIONS

The structure models which have been considered in this paper are shown in Fig. 2. As already stated in the Introduction, all of them obey Pashley's electron counting rule while being electrically neutral. No excess charges have been considered in the simulations presented in this paper.

The total energy for each of these structures was calculated in a self-consistent simulation using pseudopotentials to simulate the potential from the ion cores and a density func-
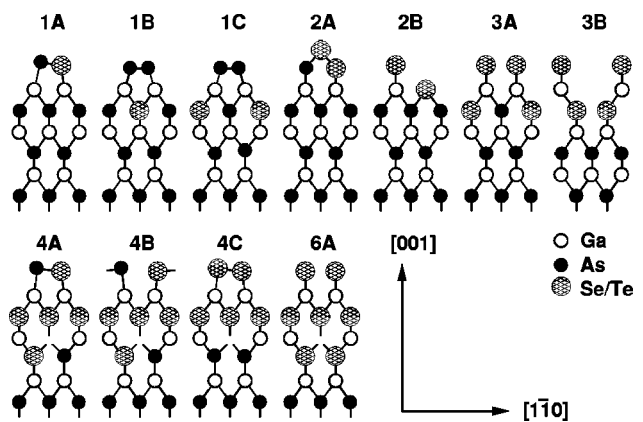

FIG. 2. Schematic ball and stick models of the structures considered in this work.

tional theory[14] (DFT) scheme to model the valence electrons. The wave functions of the valence electrons were expanded in a series of plane waves with kinetic energies up to 15 Ry. Exchange and correlation contributions to the energy of the electrons were introduced by the local density approximation (LDA) in the parametrization of Perdew and Zunger after results from Ceperley and Alder.[15] The pseudopotentials used in this work were generated following the prescription of Hamann[16] with the d component always being taken as the local potential and the separable approximation of Kleinman and Bylander[17] being applied. The integration of the charge density in reciprocal space was performed using a set of special **k** points generated by the scheme of Monkhorst and Pack.[18] Sixteen such points were used in the full reciprocal supercell. The calculations were performed with the simulation package *fhi96md* which is described in more detail in Ref. 19.

Test calculations were undertaken in order to estimate the accuracy of our parameter set. We found that upon increasing the number of **k** points from 16 to 36 the differences in total energies for different structures changed by less than 0.05 eV per 2×1 surface cell. Comparable changes were observed for different structures with equal stoichiometry for a plane wave cutoff energy of 18 Ry. In order to assert the quality of our pseudopotentials further we calculated structural properties of orthorhombic β-Ga_2Se_3. Its equilibrium lattice constant was found to be 5.37 Å, in good agreement with another theoretical study[20] and experimental data. Also the atomic displacements within the Ga_2Se_3 unit cell are similar to those shown in Ref. 20.

The supercell approach with periodic boundary conditions necessitates the simulation of a slab of atoms with vacuum between adjacent slabs whose width is sufficiently large to make interactions negligible. In our simulations one slab consisted of about ten atomic layers and the spacing of about the same thickness. Following a suggestion of Shiraishi,[21] an asymmetric slab geometry was used, the lower side being an As-terminated, unreconstructed GaAs(001) surface where the dangling bonds are passivated by hydrogenlike pseudoatoms with a nuclear charge of $Z = 0.75$ and a corresponding valence charge. This configuration removes the dangling bond states from the band gap of GaAs bulk, making the lower surface of the slab similar to bulk material. The top side of the slab exhibits the reconstructed surface with a varying amount of adsorbed Se or Te. In order to compensate for the dipole moment of the asymmetric slab an artificial dipole layer was simulated in the vacuum region between two adjacent slabs, its dipole moment being adjusted self-consistently in order to match that of the slab.

The initial atomic positions in the bulk region of the slab were chosen to be those of GaAs bulk while for dimers at the surface they were taken from Ref. 8. During the simulations the forces on all atoms save those in the lowermost GaAs layer were computed using the Hellmann-Feynman theorem[22] and adjusted until the force on each atom had decreased beneath 0.02 eV/Å. The atoms in the lowermost layers were not allowed to move from their bulk positions.

Since the amount of adsorbed chalcogen atoms per 2×1 surface cell varies in the successive calculations, it is necessary to account for the effects of varying stoichiometry on the surface energy correctly. The adsorbate-covered surfaces are assumed to be in thermal equilibrium, being able to exchange individual atoms of their constituents from appropriate reservoirs. Following an argument of Qian, Martin, and Chadi[23] the surface energy Γ is expressed as follows:

$$\Gamma = E_{\text{tot}} - \sum_i \mu_i N_i, \tag{1}$$

where E_{tot} denotes the total energy for one supercell as obtained in a simulation and μ_i and N_i the chemical potential and number of atoms of constituent i, respectively, within the supercell. While all chemical potentials are previously unknown, certain boundary conditions apply. First, the chemical potential of each constituent cannot surpass that of its most stable elemental bulk phase. Second, the chemical potential at the surface is equal to the value for the bulk beneath, since both are in thermodynamic equilibrium. This relates the chemical potential of Ga with As via the expression

$$\mu_{\text{Ga}} + \mu_{\text{As}} = \mu_{\text{GaAs}}^{\text{bulk}} = \mu_{\text{Ga}}^{\text{bulk}} + \mu_{\text{As}}^{\text{bulk}} - \Delta H_f^0(\text{GaAs}), \tag{2}$$

where $\Delta H_f^0(\text{GaAs})$ represents the heat of formation for GaAs bulk. Substituting the left-hand side of Eq. (2) into Eq. (1) leads to the expression

$$\Gamma = E_{\text{tot}} - \mu_{\text{GaAs}}^{\text{bulk}} N_{\text{Ga}} - \mu_{\text{As}}^{\text{bulk}}(N_{\text{As}} - N_{\text{Ga}}) - \mu_{\text{Se,Te}}^{\text{bulk}} N_{\text{Se,Te}}$$
$$- (\mu_{\text{As}} - \mu_{\text{As}}^{\text{bulk}})(N_{\text{As}} - N_{\text{Ga}}) - (\mu_{\text{Se,Te}} - \mu_{\text{Se,Te}}^{\text{bulk}}) N_{\text{Se,Te}}. \tag{3}$$

In this expression the differences between the chemical potential of As and Se and their respective bulk values are taken to be the variables for the graphic representation of the surface energies in Figs. 3 and 4. The lower limit of μ_{As} is fixed by the heat of formation for GaAs which was found to be 0.725 eV from self-consistent simulations. This value is in good agreement with the experimental value of 0.736 eV.[24] For the chemical potentials of Se and Te, the upper limits are given by the values of their respective bulk phases whereas for the lower limits the heat of formation for an appropriate compound has to be employed. In the case of Se the heat of formation for the compound Ga_2Se was used since its heat of formation per Se atom is higher than that of GaSe or Ga_2Se_3. Its experimentally determined value is 1.90 eV.[25] The same value was also used for the Te/GaAs system. We emphasize here that this choice is unlikely to affect the physical content of the results presented here since the most stable structure remains the same over a considerable variation of the lower limit for μ_{Te}, as can be seen from Fig. 5.

The chemical potentials of Ga, As, Se, and Te were also determined from self-consistent calculations. For Ga an orthorhombic base centered structure (A11) was assumed, for As the A7 structure as described in Ref. 26 was assumed, and for Se and Te chain structures with hexagonal symmetry were assumed. The lattice constants corresponding to the minima of the total energies for these elements deviated from those cited in the literature by less than 8% for Se and by less than 4% for all others.
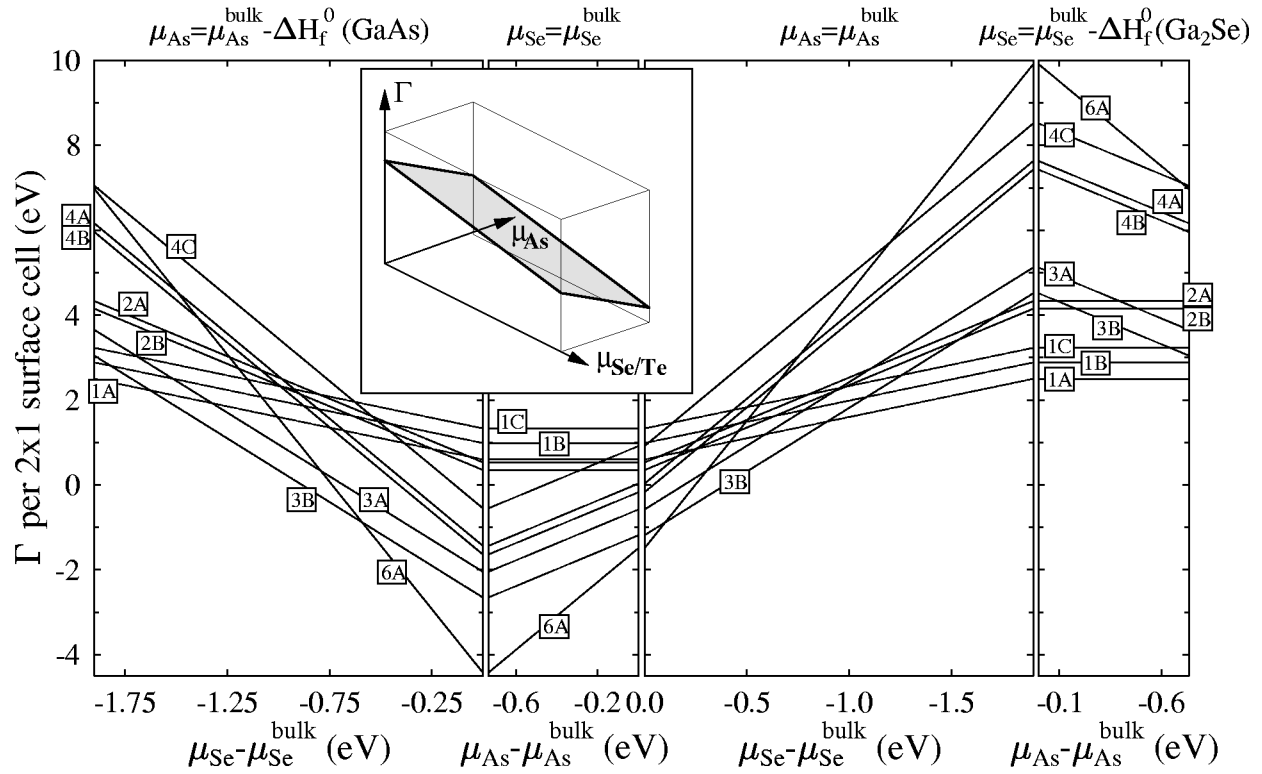
FIG. 3. Surface energies per 2×1 surface cell of the Se-adsorbed GaAs surface for the structures shown in Fig. 1. The inset gives a schematic representation of the surface energy Γ as a function of two chemical potentials.

III. RESULTS

As can be seen from Eq. (3), the surface energy Γ is a linear function of two chemical potentials which takes the shape of a plane tilted away from the ''Γ'' axis by some angle which is determined by the stoichiometry of the corresponding surface. The lines in Figs. 3 and 4 show the edges of these planes at the upper or lower limit of one chemical
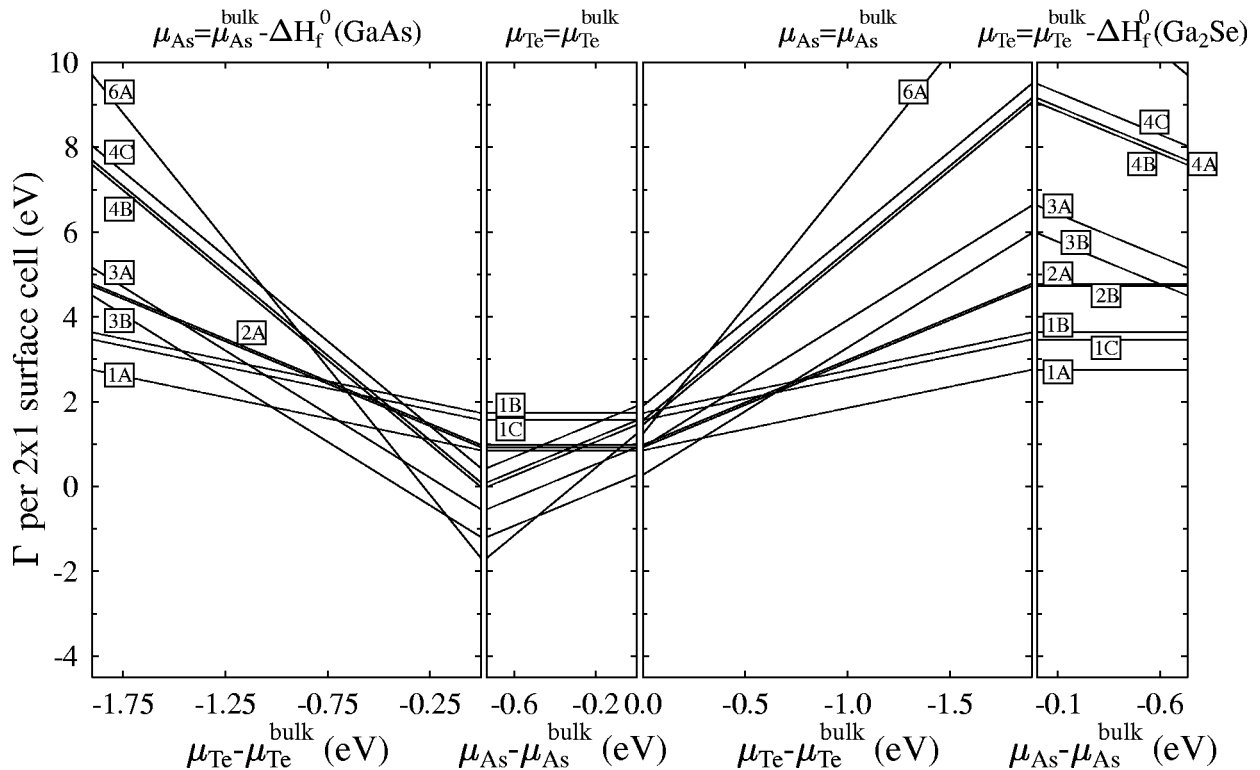

FIG. 4. Surface energies per 2×1 surface cell of the Te-adsorbed GaAs surface for the structures shown in Fig. 1.
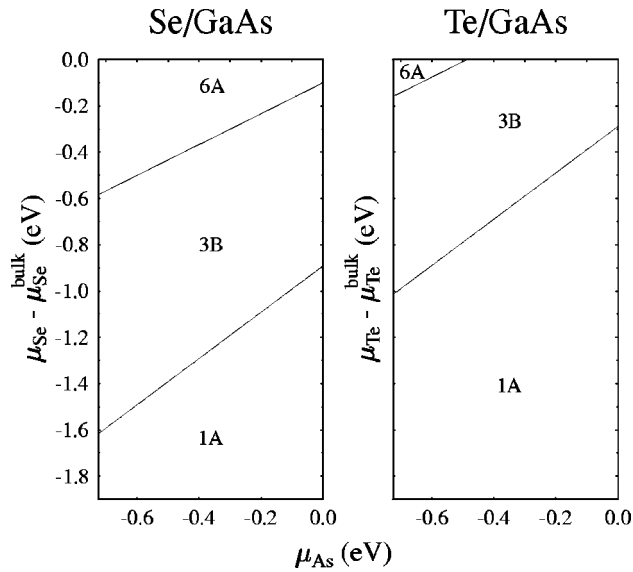
FIG. 5. The structures for Se and Te on GaAs with minimal surface energies within their respective regies of the chemical potentials of As and Se/Te.

FIG. 6. Valence charge averaged over lattice planes for structures 1A and 1B.

potential whose value appears above each graph. Each outline appears thus as a function of the remaining chemical potential. We note that in Fig. 4 the heat of formation for Ga_2Se is used to determine the lower limit of the chemical potential of Te; this is not only due to the lack of an experimental value for a suitable Ga-Te compound in the literature but also facilitates direct comparison of the two figures. The values of the involved chemical potentials over which the respective structures with minimal surface energies extend are depicted in Fig. 5.

A. The Se-adsorbed surfaces

Figure 3 shows the absolute surface energies per 2×1 surface cell computed according to Eq. (3). It can be seen that at the upper and lower limits of the As chemical potential the most stable structures remain the same while only the respective ranges of μ_{Se} differ in which they are energetically most favorable. This indicates that a variation of μ_{As} has much less effect on the structure and amount of adsorbed Se than a variation of μ_{Se}. Structure 6A, with three adsorbed monoatomic layers of Se, exhibits the largest variation of the surface energy since the effect of a change in μ_{Se} on Γ is multiplied by the number of Se atoms per 2×1 surface cell which is six in this case. By the same token this variation is least for the structures 1A, 1B, and 1C, which exhibit half of a monoatomic layer coverage of Se.

When only one Se atom per 2×1 surface cell is adsorbed, structure 1A turns out to be more stable than 1B and 1C. The preferential adsorption of one single Se atom by formation of a mixed As-Se dimer cannot be understood from kinetic aspects of the adsorption process since each surface was assumed to be in thermal equilibrium in the simulations. Assuming the strength of the Ga—Se bond to be higher than that of the As—Se bond, the Se atom should be adsorbed preferentially beneath the surface where it would be bound to four Ga atoms, instead of being bound at the surface where only two Ga—Se bonds and one As—Se bond are formed. However, adsorption beneath the top layer requires one elec-
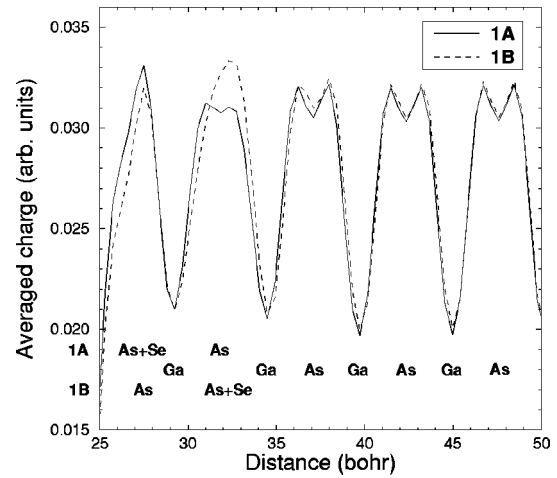
tron to be transferred from the adsorption site to the surface in order to fill all dangling bonds completely. This charge transfer can be observed for structures 1A and 1B in Fig. 6.

According to an argument of Harrison,[27] this charge transfer results in an enhanced surface dipole moment which is energetically unfavorable. We have estimated the magnitude of the dipole layers for the different structures in the following way: all atoms were assumed to carry a positive charge equivalent to their respective valence while electrons in the covalent bonds were distributed according to an assumed bond polarity of $\alpha_p = 0.5$,[27] i.e., of the two electrons that form a bond between Ga and As, 1.5 electrons were attributed to the As atom and 0.5 electrons to the Ga atom. No distinction was made between As and Se or Te, therefore a bond between either of these was assumed to be unpolarized. The charges were averaged in the atomic layers parallel to the surface in order to yield a one-dimensional charge distribution. Furthermore, relaxation of the lattice planes was assumed to be negligible. Considering the electrostatic interaction between the charged lattice planes to be screened by the dielectric constant of GaAs, which is 10.9, one obtains a potential drop of about 0.74 eV resulting from a charge density of one electron per 2×1 surface cell. From these assumptions the potential offset induced by the dipole layer at the surface of structures 1B and 1C is about 1.85 eV per 2×1 cell while the corresponding offset for structure 1A is 0.37 eV. Apparently the difference between these two energies accounts for the stability of the Se adsorption site within the mixed dimer.

Biegelsen et al.[8] report a first-principles simulation similar to that presented here for structure 1A. They find that the bond length between As and Se in the mixed dimer is about 2.49 Å while the Se atom is 0.12 Å closer to the bulk than the As atom. The respective distances from the present work are 2.50 Å and 0.21 Å. The fact that our structural data are not identical with theirs may be attributed to differences in the parameter sets and the numerical convergence of the respective simulations.

The vertical separation obtained in the present work cannot be explained from the difference of 0.04 Å between the covalent radii of As and Se alone, but can be explained by considering the difference in the ionic radii, which is 0.24
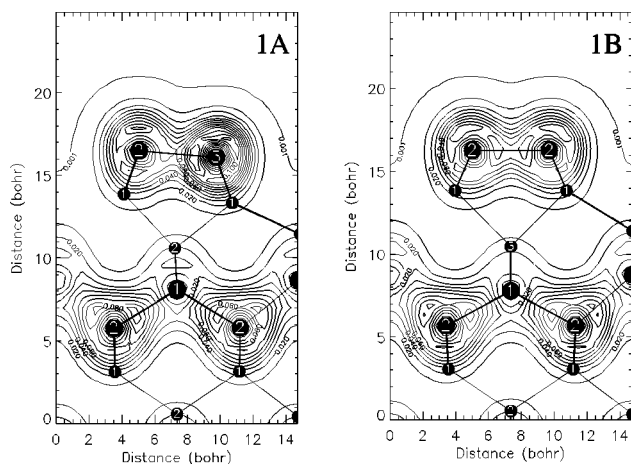
FIG. 7. Charge density contour of structures 1A and 1B. Dots labeled ''1'' refer to Ga atoms, ''2'' to As atoms, and ''3'' to Se atoms. Larger dots denote atoms that lie in the cut plane. The smaller ones denote atoms above or beneath it. Please note that positions above or beneath the cut plane are equivalent since the $\times 1$ direction of the surface reconstruction is perpendicular to the cut plane.

Å.[28] The charge density contour plot in Fig. 7 confirms this supposition since it reveals considerable charge transfer from Ga to As and from As to Se. The use of ionic radii can also be used to explain the difference in the surface energies of structures 1B and 1C: the compression of the lattice beneath the As dimer is less acute if the smaller Se atom sits beneath it.

None of the two structures with Se coverage of one atomic layer is energetically favorable compared to the others, as can be seen in Fig. 3. This is presumably due to the less stable Se—As and Se—Se bonds which are features of these structures. Charge density contours including the topmost Se atoms are shown in Fig. 8. The presence of Se—As bonds has been reported by Takatani, Kikawa, and Nakazawa[1] by means of x-ray photoelectron spectroscopy (XPS) measurements of GaAs surfaces on which Se has been deposited at room temperature, followed by an anneal at 250 °C. They also state that the adsorbed Se atoms are bound at two nonequivalent sites, which is the case for the 2A and 2B structures. Therefore either of them might occur under suitably chosen experimental conditions.

3A and 3B are the most stable structures over an intermediate range of the Se chemical potential, quite irrespective of
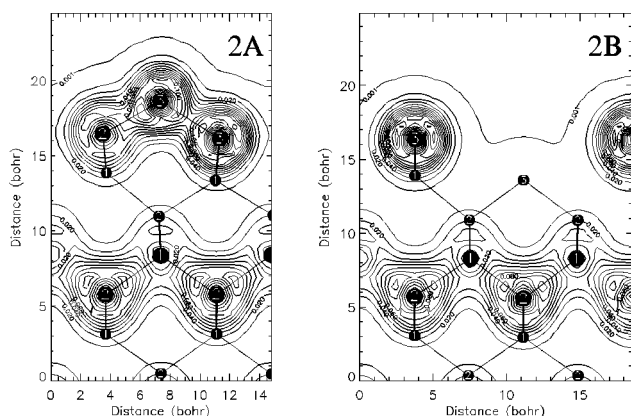

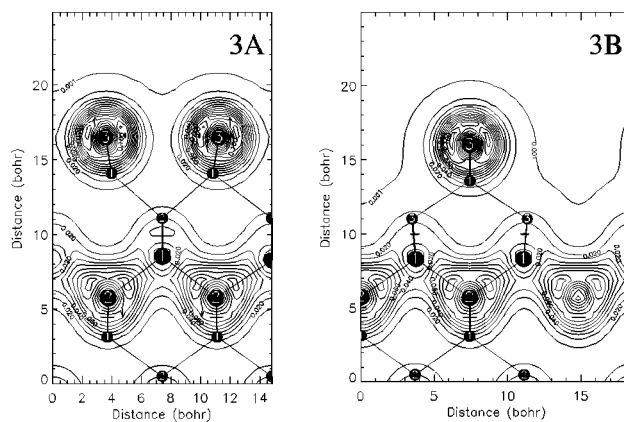FIG. 8. Charge density contour of structures 2A and 2B.

FIG. 9. Charge density contour of structures 3A and 3B.

that of As. Both structures feature Se atoms in the top atomic layer which reside in bridge positions and are disconnected from each other. Since the dangling bonds of the Se atoms are completely filled there is no driving force for dimerization, as can be conceived from Fig. 9. The enhanced stability of structure 3B with respect to 3A may be explained from two observations. In the first place relaxation of the atoms in the first atomic layers beneath the surface may occur more easily since the surface atoms are less tightly bound. Second, an estimation of the potential offset due to a surface dipole layer as described above reveals a difference of about 0.74 eV per 2×1 surface cell in favor of structure 3B. This estimated difference is already quite close to the actual difference in the surface energies of 0.61 eV between structures 3A and 3B. Therefore the enhanced stability of structure 3B may be readily explained by the magnitude of the surface dipole. Since in both structures the surface is terminated entirely by completely filled Se dangling bonds it should be quite resistant to further adsorption of atoms on top of it; therefore these structures could explain the three-dimensional growth mode of ZnSe on a previously Se-terminated GaAs(001) surface.[29,30]

The adsorption of two complete atomic layers of Se on GaAs requires the formation of a Ga vacancy beneath the surface in order to counterbalance the increased number of electrons introduced by the Se atoms. Within the 2×1 reconstruction the vacancies form channels extending in the [110] direction. The electrostatic interaction of the filled dangling bonds that protrude into these channels will presumably raise the surface energies of such structures, thus rendering them less stable. The charge accumulation around the Ga vacancy can be seen in Fig. 10 where two slices of structure 4A are plotted such as to provide charge contours around all atoms situated near the vacancy. The stability of structures with Ga vacancies buried beneath the surface stems mainly from the superior strength of the Ga—Se bonds that are formed by incorporation of Se atoms on As sites. The adsorption of four Se atoms per 2×1 cell requires the formation of a surface dimer from electron counting considerations. This dimer can either be a mixed one or consist entirely of Se atoms; the case of Se incorporation beneath a pure As dimer was not considered in this work since the experimental investigations cited in the Introduction agree with the observation that the Se concentration should be highest at the surface and decrease in the layers beneath; in
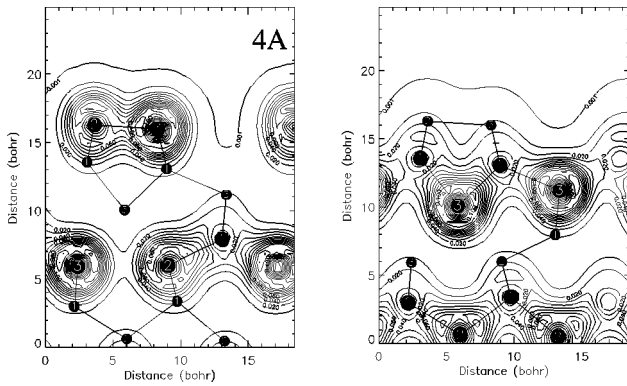
FIG. 10. Charge density contours of structure 4A. The left-hand plot includes the surface dimer and the two atoms below the Ga vacancy. The right-hand plot features the cut plane defined by those atoms that lie outside the plane shown in the left-hand panel (i.e., those denoted there by the smaller dots).

FIG. 11. Charge density contour plots of structure 6A. The cut planes were chosen similar to those for the plots of structure 4A.

addition the estimated surface dipole potential offset of such a structure surpasses that of structures 4A and 4B by 2.2 eV per 2×1 cell.

From Fig. 3 it can be seen that structure 4C, which features the pure Se dimer in the top layer, is even less stable than structures 4A and 4B with the mixed dimer on top. The potential offset estimated from the surface dipole moment is 3.3 eV per 2×1 cell for structure 4C as opposed to 0.37 eV for 4A and 4B. From our simulations we find that the difference between the surface energies of 4C and 4A (or 4B) is only about 1 eV. While this inconsistency reveals the shortcomings of our approximation, we believe that the qualitative information that can be derived from it sufficiently explains the inferior stability of structure 4C with respect to 4A and 4B.

Since structure 4C has been proposed explicitly as a structural model for the Se-adsorbed GaAs(001) surface from scanning tunneling microscope (STM) investigations, e.g., by Pashley and Li,[10] the question arises as to how the apparent instability of this structure can be made congruent with the experimental evidence presented in Ref. 10. We propose that structure 3B rather than one of the structures 4A, 4B, or 4C is the microscopic structure that is realized on a GaAs(001) surface with a moderate amount of Se being adsorbed. While the unperturbed valence charge is strongly localized around the Se atoms in the top layer of structure 3B, as is shown in Fig. 9, a high sample bias might instead result in a broadening of the charge around the Se atoms in the vicinity of the tunneling tip. Of course the question of the real microscopic structure cannot be decided from our simulation data alone. Nevertheless, we would like to stress the point that structure 3B is in reasonable agreement with the experimental evidence concerning the amount of adsorbed Se and the observation of two nonequivalent bonding sites in addition to its surface energy being the lowest of all structures considered in this work over an intermediate range of the Se chemical potential.

With the adsorption of three atomic layers of Se on a GaAs(001) surface one gets close to the growth of strained Ga_2Se_3 on GaAs. Because of electron counting considerations only one structure for three adsorbed layers of Se can be conceived. While 6A appears to be the most stable structure at the upper limit of the chemical potential of Se, the
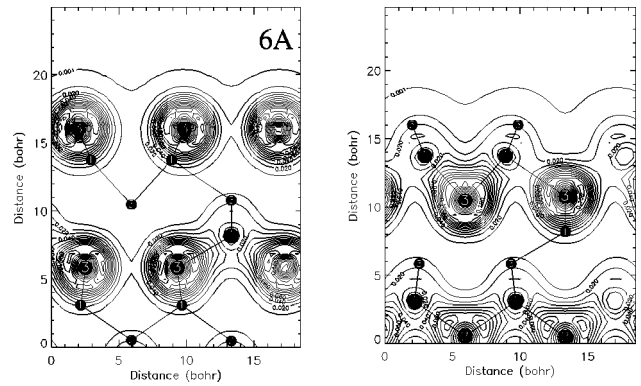
amount of adsorbed Se surpasses significantly that observed in the experiments reviewed in the Introduction. The number of excess electrons introduced by the Se atoms requires the surface Se atoms to reside at bridge positions without the formation of a surface dimer in order to meet Pashley's electron counting rule. The surface is therefore similar to that of structure 3A. Its relative stability is probably also due to the comparatively small distortion that results from the absence of a surface dimer. The effect of the massive Se adsorption results in a surface dipole potential offset of about 2.6 eV which is only 0.74 eV lower in magnitude than that of structure 4C, as estimated from the model described above. Two charge contours similar to these of structure 4A are shown in Fig. 11.

The structures 4A–4C and 6A share a high density of Ga vacancies just beneath the surface. To our knowledge such a defective structure has not yet been observed on Se-reacted GaAs(001) surfaces. On the other hand, Li *et al.* have reported transmission electron microsope (TEM) studies of Ga_2Se_3 (Ref. 31) and ZnSe (Ref. 32) grown epitaxially on GaAs. In both cases a Ga_2Se_3-like transition structure is observed that contains a large number of vacancies in order to maintain stoichiometry. In the latter case the thickness and composition of the transition layer proposed in Ref. 32 suggest structure 3B as the most likely precursor, supposing that no atoms desorb from the surface during the ZnSe growth start.

B. The Te-adsorbed surfaces

In the case of half a monoatomic layer adsorption of Te on GaAs the preferred adsorption site is the same as in the case of Se adsorption while the absolute surface energy is about 0.5 eV higher, as can be seen from Fig. 4. We attribute this increase in the surface energy to the inferior strength of the Ga—Te bond compared to the Ga—Se bond. This tendency has already been predicted, e.g., by Ohno.[12] We note in addition that in the mixed dimer of structure 1A the Te atom sits about 0.02 Å closer to the GaAs bulk than the As atom. The covalent radii of As and Te are insufficient to explain this configuration since the latter is 0.11 Å larger than the former.[28] Considering ionic instead of covalent atomic radii one finds that the radius of Te is 0.01 Å smaller than that of As. Therefore one may assume the Ga—Te bond to be considerably polarized. The charge density contours shown in Fig. 12 confirm this supposition. Furthermore, the
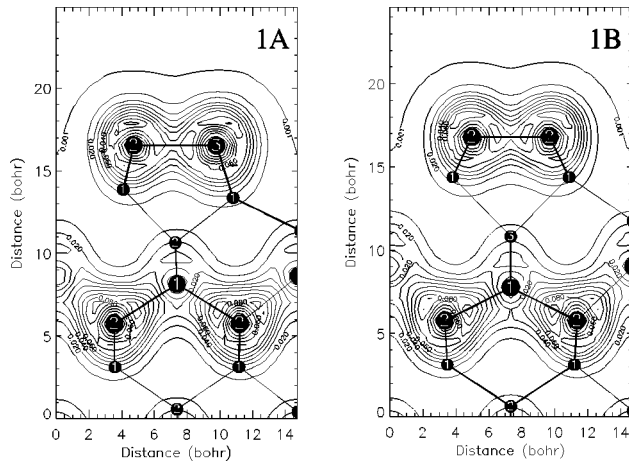
FIG. 12. Charge density contours for structures 1A and 1B with one Te atom per unit cell being adsorbed. Labels ''1,'' ''2,'' and ''3'' refer to Ga, As, and Te atoms, respectively.

structures 1B and 1C have become almost equal in energy. We attribute this also to the radius of the Te atom; if it is almost equal to that of As there is no longer any distinction between structures 1B and 1C as far as the lattice distortion in the first planes at the surface is concerned.

For the structures 2A and 2B, the upward shift of the surface energies is similar to that of structure 1A. Since the same number of Ga— Se bonds are replaced by Ga—Te bonds in each case, this shift can be readily explained by considering the different strengths of the Ga—chalcogen bonds.

Similar to the case of Se adsorbed on GaAs, the structures 3A and 3B are those with the lowest surface energies over an intermediate range of the chemical potential of Te. Compared to the former case their energies are shifted by about 1.5 eV towards higher values. Nevertheless, the relative difference in energies of the two structures 3A and 3B does not change noticeably. This observation can be explained by assuming the difference in bond strength between Ga— Se and Ga—Te to be about 0.15 eV. If one assumes a similar difference for the As—Se and As—Te bonds there is also overall agreement with the energy shifts of structures 1A through 2B; this assumption is supported by the data in Ref. 12. It should also be noted that the contour lines around the topmost Te atoms in Fig. 13 are less dense than those around the
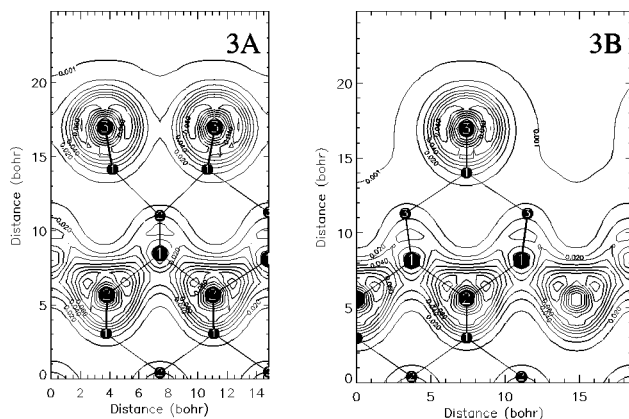

FIG. 13. Charge density contours of structures 3A and 3B for the Te-reacted surfaces.

Se atoms in Fig. 9, due to the lower electronegativity of Te with respect to Se.

Recently precise atomic positions for Te-adsorbed GaAs surfaces have been determined in an x-ray standing wave experiment by Sugiyama and Maeyama.[7] From their results they conclude that the Te atoms preferentially occupy As sites and form Te—Ga bonds. Furthermore, they report two different separations between the Te atoms and the Ga atoms in the lattice planes below. While this vertical spacing is about 1.69 Å for Te atoms in the first position from both views along the (111) and ($1\bar{1}1$) diffraction planes, there is considerable disagreement in their data for the Te atoms in the second position, the vertical separations being 2.13 Å and 2.45 Å for the (111) and ($1\bar{1}1$) diffraction planes, respectively. Comparing these data with the relaxed atomic positions obtained from our simulations of structures 3A and 3B, we find that the vertical separations between the Te atoms in the third lattice planes and the Ga atoms beneath agree well with the reported value of about 1.69 Å, being 1.70 Å and 1.68 Å for structures 3A and 3B, respectively. The respective separations between Te atoms in the top layers and Ga atoms in the second layers are 1.52 Å and 1.58 Å, thus agreeing less well with the data from Ref. 7.

We point out that the distances between Te atoms in the top layers and Ga atoms below are generally lower than those for the Te atoms in the third lattice plane. This circumstance can be understood in light of the rearrangement of valence electrons that is required for the surface to agree with Pashley's counting rule; the excess electrons from chalcogen atoms buried in the GaAs bulk have to be transferred to the surface where they can eventually fill partially empty dangling bonds. The surface dipole moment thus formed does in all probability attract the surface atoms to the bulk. From this argument we see no reason why the Te atoms in bridge positions at the surface should be located at a greater distance from the first Ga lattice plane than the Te atoms in the plane below, as is suggested by Sugiyama and Maeyama. We have performed an additional simulation for a structure similar to 3B but with the Te atom in the top layer residing in an on-top position above one Ga atom. For this structure we find that the vertical separation between these two atoms is about 2.29 Å which is the average of the two distances reported by Sugiyama and Maeyama. However, the surface energy of this structure is about 1.76 eV above that of structure 6A, thus rendering the adsorption of the Te atom at the on-top site to be energetically extremely unfavorable. This difference in energies considerably exceeds the value of 1.27 eV reported by Ohno.[12] Therefore the origin of the large vertical separation between some of the Te atoms and the underlying Ga atoms reported in Ref. 7 cannot be determined here.

For the GaAs surfaces covered with two atomic layers of Te, one observes a shift towards higher surface energies, compared to the case of Se adsorption, which is about 1.5 eV for the structures 4A and 4B but only about 1.0 eV for structure 4C. This means that the energy separation between structure 4C and structures 4A and 4B decreases. We think that this behavior can be explained by the lower electronegativity of Te, as compared to Se, which also results in a lower surface dipole moment, rendering the present structure 4C energetically less unfavorable.
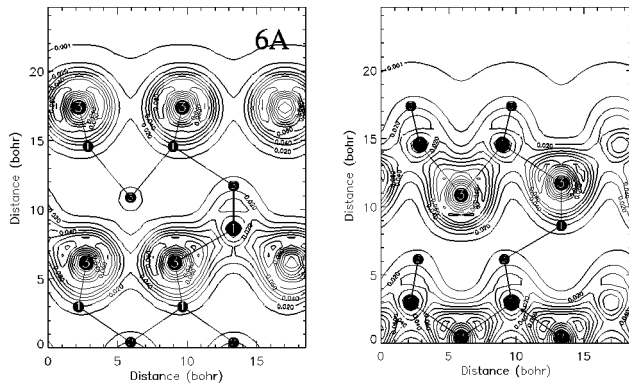
FIG. 14. Two charge density contours for structure 6A showing the charge distribution around the Ga vacancy.

In the case of three atomic layers of adsorbed Te, the surface energy increases sufficiently to prevent structure 6A from becoming the energetically most favorable one except for a narrow range around the upper limit of μ_{Te} and the lower limit of μ_{As}. One obvious reason for this is the larger atomic radius of Te which becomes manifest in the observation that while the Se atoms in the top layer are shifted 0.1 Å towards the GaAs bulk, the Te atoms in the present case are moved 0.6 Å away from it towards the vacuum. Also the charge around the Te atoms around the Ga vacancy is less localized than for the same structure with Se instead of Te atoms, thus probably raising the electrostatic interaction between these bonds. This can be inferred from Fig. 14. We state furthermore that the 3 eV shift of the surface energy of structure 6A may also be explained by the different strengths of the Ga—Se and Ga—Te bonds as outlined above; attributing a difference of 0.15 eV to these bond strengths would account for a shift of 2.4 eV of the surface energy for a 2 ×1 cell. From this argument it appears that only a minor fraction of the observed total shift may actually be attributed to the elastic distortion of the first lattice planes at the surface.

Recently the growth start of ZnSe on a previously Te-treated, well-ordered surface has been investigated by Ohtake *et al.*[33,34] Starting from a 6×1 reconstructed Te/GaAs surface they notice that while layer-by-layer growth of the ZnSe film can be accomplished, an extraordinarily high density of stacking fault defects occurs. Speculating that the 6×1 surface cell of Te adsorbed on GaAs is probably formed out of three instances of the energetically most favorable structures reported in this work, the arguments concerning the passivation of the Se-adsorbed GaAs surface presented above apply here as well and might sufficiently explain the creation of stacking faults. The authors state furthermore that about 1.2 atomic layers of Te remain at the GaAs-ZnSe interface in their growth experiment, forming a thin Ga_2Te_3-like interface layer. This quantity agrees reasonably well, for example, with the amount of Te adsorbed on GaAs in the structures 3A and 3B whereas the observation of empty sites at the interface would render a structure similar to 3B the most promising candidate for the initial surface composition. Of course a more Te-rich structure such as 6A could be formed initially, while after the ZnSe growth start a certain amount of Ga and Te desorbs. However, the average

coverage of 0.8–1.0 atomic layers reported in the literature[5,6] for the Te-adsorbed GaAs(001) surface renders this alternative less probable.

IV. SUMMARY AND CONCLUSION

The surface energies of various Se- and Te-adsorbed GaAs(001) surfaces exhibiting 2×1 reconstruction have been determined from first-principles simulations. The structures evaluated in these calculations were derived from the available experimental data for these surfaces. The surface energies were evaluated as functions of the chemical potentials of the concerned species. Therefore the relative stabilities of the investigated structures are determined in terms of ambient conditions that might typically occur during the fabrication of samples as summarized in the Introduction.

From our calculations we conclude that chalcogen atoms adsorbed on GaAs(001) show little tendency to form surface dimers. Instead, the most stable surface site is the bridge site where the surface chalcogen atom is bound to two Ga atoms in the layer beneath. Despite considerable differences in the surface energies for Se and Te the behavior of these two species is qualitatively similar.

Due to strict adherence to the electron counting rule no surface charge accumulation could occur for any of the structures investigated in this work. It could be shown that in its absence surface dipole layers are a key feature for the stability of adsorbate structures. From integration of Poisson's equation for simple models of the actual structures their differences in energies could be asserted in part even quantitatively. Differences in stability between similar structures upon the exchange between Se and Te could be attributed mainly to the different strengths of the Ga—Se and Ga—Te bonds.

The structural information derived from our calculations was compared with experimental results. It was found that the structures that appear to be most stable from our calculations agree well with the available experimental data. Bonding sites, surface stoichiometry, and bond lengths reported in the literature are mainly confirmed by our results. In addition they offer an explanation for the evolution of highly defective transition structures that appear during the growth of ZnSe on previously chalcogen-exposed GaAs(001) surfaces.

It is beyond the scope of calculations like ours to model the highly complex process of adsorbate formation that obviously depends strongly on details of the sample preparation and ambient conditions. Also surfaces prepared in such ways will be much more complex than our model structures can account for. We expect that different structures will form a mixture of phases which will be stabilized by the increase of disorder on the surface. The most stable structures presented in this work may be considered as basic units of which the real surfaces are formed.

*Electronic address: gundel@physik.uni-wuerzburg.de

[1] S. Takatani, T. Kikawa, and M. Nakazawa, Phys. Rev. B **45**, 8498 (1992).

[2] T. Scimeca, Y. Watanabe, R. Berrigan, and M. Oshima, Phys. Rev. B **46**, 10 201 (1992).

[3] D. Li and M. D. Pashley, Phys. Rev. B **49**, 13 643 (1994).

[4] S. A. Chambers and V. S. Sundaram, J. Vac. Sci. Technol. B **9**, 2256 (1991).

[5] Y. Gobil, J. Cibert, K. Saminadayar, and S. Tatarenko, Surf. Sci. **211/212**, 969 (1989).

[6] V. H. Etgens, R. Pinchaux, M. Sauvage-Simkin, J. Massies, N. Jedrecy, N. Greiser, and S. Tatarenko, Surf. Sci. **251/252**, 478 (1991).

[7] M. Sugiyama and S. Maeyama, Phys. Rev. B **57**, 7079 (1998).

[8] D. K. Biegelsen, R. D. Bringans, J. E. Northrup, and L.-E. Swartz, Phys. Rev. B **49**, 5424 (1994).

[9] W. Spahn, H. R. Reß, C. Fischer, R. Ebel, W. Faschinger, M. Ehinger, and G. Landwehr, in *Physics and Simulation of Optoelectronic Devices IV*, edited by W. W. Chow and M. Osiński [Proc. SPIE **2693**, 10 (1996)].

[10] M. D. Pashley and D. Li, J. Vac. Sci. Technol. A **12**, 1848 (1994).

[11] M. D. Pashley, Phys. Rev. B **40**, 10 481 (1989).

[12] T. Ohno, Surf. Sci. **255**, 229 (1991).

[13] W. A. Harrison, *Electronic Structure and the Properties of Solids* (Dover, New York, 1989).

[14] P. Hohenberg and W. Kohn, Phys. Rev. **136**, B864 (1964); W. Kohn and L. J. Sham, *ibid.* **140**, A1133 (1965).

[15] J. P. Perdew and A. Zunger, Phys. Rev. B **23**, 5048 (1981); D. M. Ceperley and B. J. Alder, Phys. Rev. Lett. **45**, 566 (1980).

[16] D. R. Hamann, Phys. Rev. B **40**, 2980 (1989).

[17] L. Kleinman and D. M. Bylander, Phys. Rev. Lett. **48**, 1425 (1982).

[18] H. D. Monkhorst and J. D. Pack, Phys. Rev. B **13**, 5188 (1976).

[19] M. Bockstedte, A. Kley, J. Neugebauer, and M. Scheffler, Comput. Phys. Commun. **107**, 187 (1997).

[20] M. Peressi and A. Baldereschi, J. Appl. Phys. **83**, 3092 (1998).

[21] K. Shiraishi, J. Phys. Soc. Jpn. **59**, 3455 (1990).

[22] R. P. Feynman, Phys. Rev. **56**, 340 (1939).

[23] G.-X. Qian, R. M. Martin, and D. J. Chadi, Phys. Rev. B **38**, 7649 (1988).

[24] *CRC Handbook of Chemistry and Physics*, edited by D. R. Lide (CRC Press, Boca Raton, 1994).

[25] *Gmelin Handbuch der Anorganischen Chemie*, 8th ed., edited by H. K. Kugler (Springer, Berlin, 1981).

[26] R. J. Needs, R. M. Martin, and O. H. Nielsen, Phys. Rev. B **33**, 3778 (1985).

[27] W. A. Harrison, J. Vac. Sci. Technol. **16**, 1492 (1979).

[28] C. Kittel, *Einführung in die Festkörperphysik*, 9th ed. (Oldenbourg, München, 1991).

[29] D. Li and M. D. Pashley, J. Vac. Sci. Technol. B **12**, 2547 (1994).

[30] W. Spahn, H. R. Reß, K. Schüll, M. Ehinger, D. Hommel, and G. Landwehr, J. Cryst. Growth **159**, 761 (1996).

[31] D. Li, Y. Nakamura, N. Otsuka, J. Qiu, M. Kobayashi, and R. L. Gunshor, J. Vac. Sci. Technol. B **9**, 2167 (1991).

[32] D. Li, J. M. Gonsalves, N. Otsuka, J. Qiu, M. Kobayashi, and R. L. Gunshor, Appl. Phys. Lett. **57**, 449 (1990).

[33] A. Ohtake, L. H. Kuo, T. Yasuda, K. Kimura, S. Miwa, and T. Yao, J. Vac. Sci. Technol. B **15**, 1254 (1997).

[34] A. Ohtake, L.-H. Kuo, K. Kimura, S. Miwa, T. Yasuda, C. Jin, T. Yao, N. Nakajima, and K. Kimura, Phys. Rev. B **57**, 1410 (1998).